

Effect of the Heat Treatment Time on the Characteristics of the Coating Formed on Nanocrystalline Finemet Foils

Sima Mirzaei*, Ali Jazayeri Gharehbagh

Materials Research Center, Technology Development Institute, Sharif Branch of ACECR, Tehran, Iran,

ARTICLE INFO

Article history:

Received 11 November 2016
Accepted 14 Nov February
Available online 1 April 2016

Keywords:

Planar Flow Casting (PFC)
Process
Nanocrystalline Foil
Finemet
Insulating Coating
Magnetic Core

ABSTRACT

In the present research, amorphous $\text{Fe}_{73.5}\text{Si}_{13.5}\text{B}_9\text{Nb}_3\text{Cu}_1$ Finemet foils with 21-26 μm in thickness and 5mm in width were prepared by Planar Flow Casting (PFC) process. Wound cores of amorphous Finemet foils were simultaneously annealed and heat treated at 540°C for 60, 120 and 240 minutes in steam and air flow to form an oxide insulating coating layer on both surfaces of the foils. The structure of nanocrystalline foils was examined by X-ray diffractometry (XRD). The thickness and chemical composition of the insulating coating layer were studied by Field Emission Scanning Electron Microscopy (FE-SEM), Grazing Incidence XRD (GI-XRD), and Fourier Transform Infrared Spectroscopy (FTIR). The results show that the coating thickness formed on air and wheel surfaces of the foil was in the range of 65-310 nm and these thin coating layers contain a mixture of iron, silicon, boron, and niobium oxides. The study of magnetic properties in amorphous and nanocrystalline states revealed that nanocrystalline cores have superior soft magnetic properties compared with the amorphous ones. In other words, heat treatment gives rise to a decrease in hysteresis loss and a significant increase in saturation induction and magnetic permeabilities.

1. Introduction

Nanocrystalline soft magnetic alloys were first introduced by Yoshizawa et al. in 1988 [1]. Among different nanocrystalline alloys, Fe-Si-B-Nb-Cu alloys (i.e. Finemet) have attracted much interest because of their excellent soft magnetic properties which are related to their nanocomposite microstructure (i.e., Fe-Si crystallites within an amorphous matrix). The combination of low magnetostrictive coefficient and large saturation magnetization in an Fe-based alloy has provided an exciting advance for the field of soft magnetic alloys, and despite the formation of crystallites in the alloy, the

magnetocrystalline anisotropy is remained low, as exemplified by the small coercivity. It was later revealed that these improved properties were possible when grain sizes were less than ~15 nm and there was a sufficient exchange coupling between grains (described by the Random Anisotropy Model) [2]. Owing to their outstanding soft magnetic properties, nanocrystalline Finemet ribbons/foils have found extensive applications in transformer cores, chokes, and magnetic sensors. Using these materials in transformer cores gives rise to the core loss reduction of about 70% compared to the conventional silicon steels.

* Corresponding Author:
Email: s_mirzaei1@yahoo.com

Toroidal transformer cores are made by winding thin ribbons/foils tightly to form a multi-layered lamination. For high frequency applications (i.e. greater than 400Hz), the individual layers of a wound magnetic core must be electrically insulated. Without such insulation, the core has properties similar to a large metal block at high frequencies and will experience great power losses due to eddy currents [3]. Selection of the insulation material is governed by some criteria, such as a difference between thermal expansion coefficients of the metal and the insulating materials. The thermal expansion coefficient difference significantly affects the magnetic performances of the final cores [4].

Many insulating methods have been proposed for nanocrystalline ribbons/foils. Comparative studies showed that the most suitable method recently used by core manufacturers, to attain highly uniform, controllable thin coatings on Finemet ribbons/foils, is the oxidizing of a multi-layered core in a mixture of steam and oxygen atmosphere [5]. The method includes exposing of magnetic core to steam in the presence of air (~20% O₂) at elevated temperatures to form insulating layers on both surfaces of the foils in the wound core. Schematic drawings of a wound core before and after the formation of the insulating layer are illustrated in Fig. 1. The steam and heat accelerate the electron transfer rate from elements to oxygen to form the oxides [3].

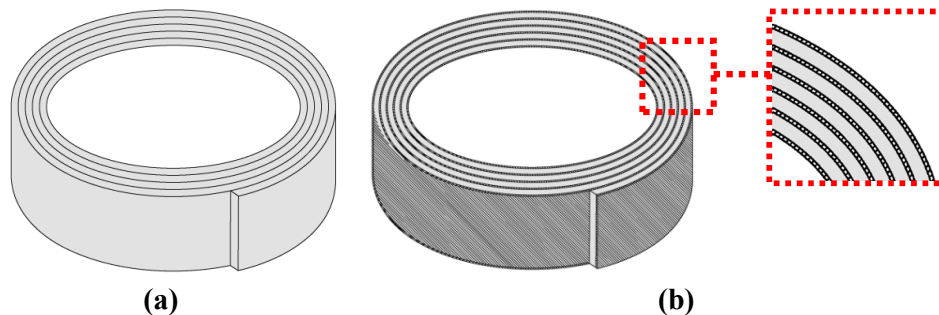


Fig 1. Schematic view of a toroidal wound core; a) prior to formation of the insulating layer, b) after formation of the insulating layer

Many researches have been done in the field of preparation and characterization of small-width Finemet type ribbons [6, 7] and a few works have been published concerning wide Finemet ribbons [8] during the last decade; but, to our knowledge, no empirical research has been done on the formation of insulating coating on Finemet ribbons/foils in Iran.

In the present work, amorphous Finemet foils are prepared by Planar Flow Casting (PFC) process and the effect of simultaneous annealing and oxidation process on the coating characteristics formed on nanocrystalline foils is reported for the first time in Iran. The effect of insulating coating on soft magnetic properties of the prepared magnetic wound core is discussed as well.

2. Experimental Procedure

Finemet alloy of nominal composition Fe_{73.5}Si_{13.5}B₉Cu₁Nb₃ was prepared by induction melting in argon atmosphere using high purity elements. The amorphous foils, 5mm in width and 20-30μm in thickness, were produced by Planar Flow Casting (PFC) process under nitrogen atmosphere using a BN nozzle with a rectangular slit (Fig. 2). The ejection pressure was fixed at 700 mbar and other processing parameters were varied in a limited range (i.e. wheel speed: 25-26 m/s, nozzle-wheel gap: 160-180μm).

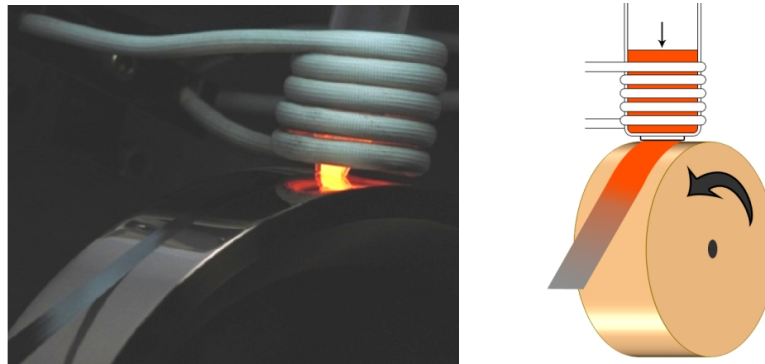


Fig 2. Schematic view and real image of Planar Flow Casting process [9]

The crystallization temperature of amorphous alloys was evaluated with a differential scanning calorimeter (DSC) at a heating rate of $10^{\circ}\text{C}/\text{min}$ under N_2 flow. The wound cores of amorphous Finemet foils (ID: 15mm, OD:20mm) were simultaneously annealed and treated with steam and air at 540°C (according to DSC measurement) for 60, 120 and 240 minutes to form oxide insulating coating on both surfaces of the adjacent foil layers of the cores. The prepared toroidal wound core and schematic illustration of the system used for simultaneous annealing and oxidation experiments of the cores are shown in Fig. 3.

The structures in the as-quenched and annealed states were studied by X-ray diffractometry (XRD) and the average grain size was estimated using the Scherrer formula. The surface morphology of the oxidized foils was examined using optical microscopy. The thickness and chemical composition of the insulating coating were studied by Field Emission Scanning Electron Microscopy (FE-SEM, MIRA3 TESCAN), Grazing Incidence XRD (GI-XRD, X'pert Pro MPD) and Fourier Transform Infrared Spectroscopy (FTIR, Bruker Tensor 27). Soft magnetic properties of the toroidal wound cores (Fig. 3b) were measured using a dc B-H loop tracer (MATS-2010S).

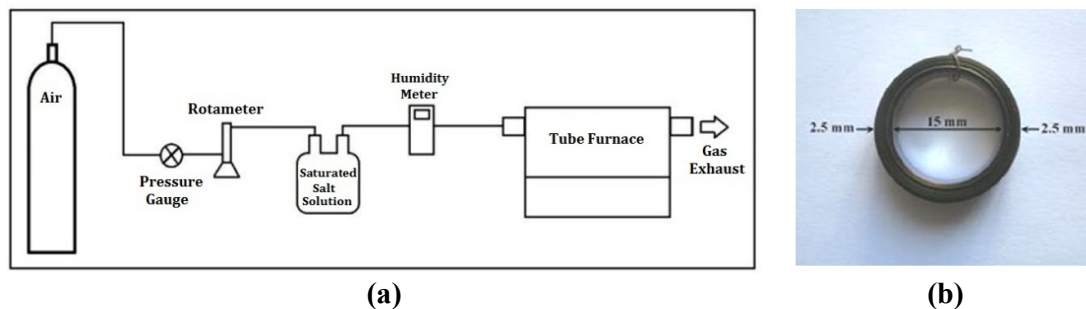


Fig 3. a) Schematic illustration of the system used for simultaneous annealing and oxidation tests, b) toroidal wound core

3. Results and Discussion

3.1. Production of Amorphous Foils via Planar Flow Casting Process

Fig. 4 shows the $\text{Fe}_{73.5}\text{Si}_{13.5}\text{B}_9\text{Cu}_1\text{Nb}_3$ foil produced in this research with a width of 5 mm and a thickness of 21-26 μm . As can be observed,

the as-cast foil has a high ductility which is a great advantage in industrial applications.

Fig. 5 presents multiplot XRD patterns for the contact and free sides of the as-cast foil. As can be seen, the XRD patterns for the as-quenched foil exhibit only one broad peak around $2\theta \approx 45^{\circ}$, which is often known as diffuse halo, indicating that the as-quenched foil is fully amorphous

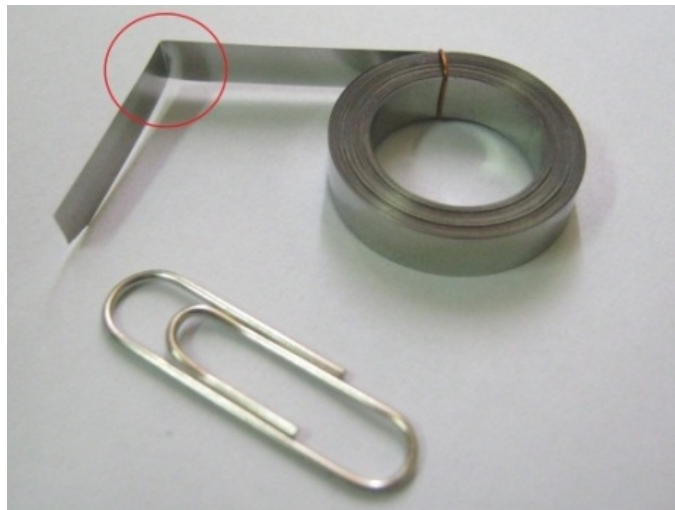


Fig.4. The as-quenched $\text{Fe}_{73.5}\text{Si}_{13.5}\text{B}_9\text{Cu}_1\text{Nb}_3$ foil produced in this research

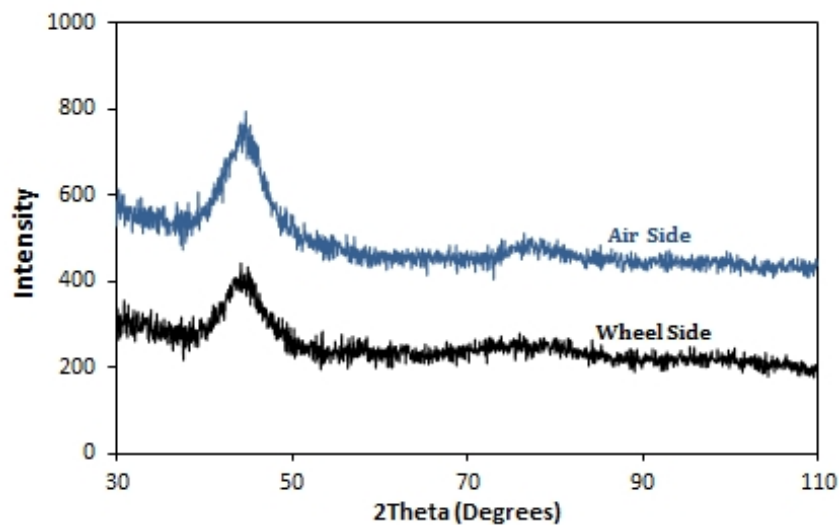


Fig 5. XRD multiplot patterns of the contact and free sides of the as-cast foil

3.2. Simultaneous Nanocrystallization and Insulating Process

The heat treating temperature for simultaneous nanocrystallization and insulating process was determined based on Differential Scanning Calorimetry (DSC) results. Fig. 6 shows the DSC curve of the as-cast amorphous foils obtained at a $10^\circ\text{C}/\text{min}$ heating rate. As can be seen, two strong exothermic peaks were detected, the first peak is at about 542°C and the

second one is at about 692°C . The peak appearing at around 551°C is attributed to the primary crystallization of the nanocrystalline phase, i.e., $\text{Fe}(\text{Si})$ soft ferromagnetic phase, and the other one at $\sim 691^\circ\text{C}$ is related to the formation of iron boride phase/s [6, 10]. Since the first peak is attributed to the formation of soft ferromagnetic nanocrystalline Fe-Si phase, the heat treatment temperature was chosen to be 540°C .

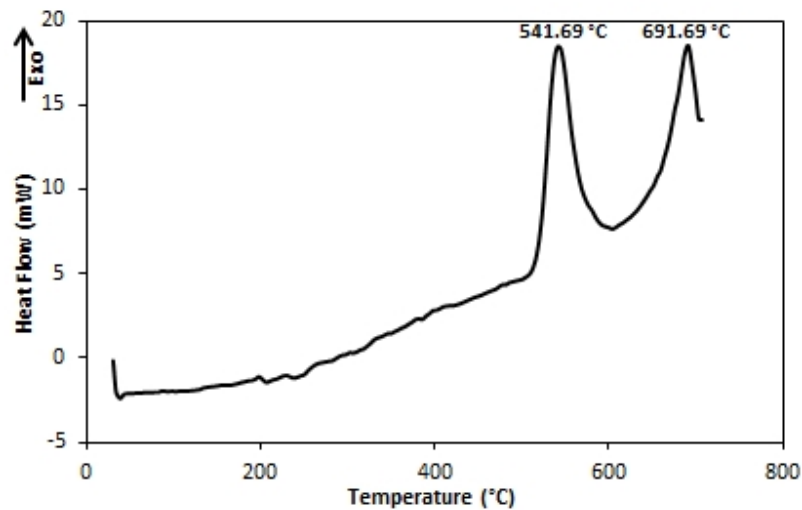


Fig 6. DSC curve of the as-cast amorphous foil measured at a heating rate of $10^{\circ}\text{C}/\text{min}$

3.3. Characterization of the Coating Layers

Simultaneous annealing and oxidation process at various conditions, i.e. different gas flow rates, gas pressures and heat treatment times, gave rise to the appearance of different colors in both surfaces of the foils. Analysis of the results

revealed that the most important parameter in the appearance of certain colors is the heat treatment time. Fig. 7 compares the optical images taken from the wheel surface of the as-cast foil with the simultaneously annealed and coated foils for various times.

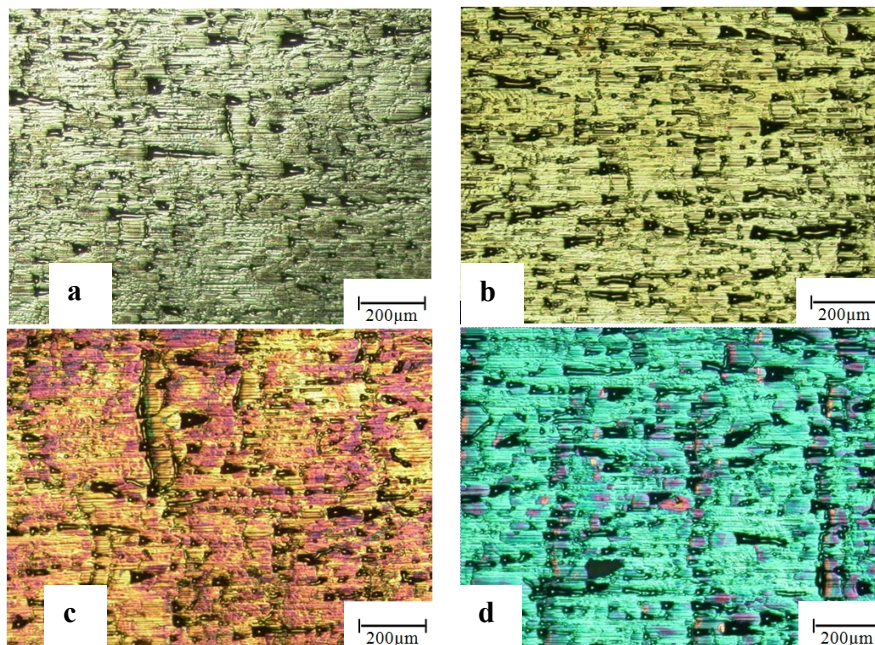


Fig 7. Optical image of the contact surfaces of a) the as-cast foil; and simultaneously annealed and coated foils for: b) 60 minutes, c) 120 minutes, d) 240 minutes

All images, presented in Fig. 7, have surface defects such as air pockets. The air pockets are randomly distributed on the wheel contact

surface of the foils and originate from the entrapment of air during the production of foils by PFC process [11].

Fig. 8 presents XRD multiplot patterns of the simultaneously annealed and coated samples for 60, 120 and 240 minutes. These patterns clearly indicate the formation of Fe_3Si crystals. The

average grain size (d) of Fe_3Si phase was found to be in the range of 10 to 12nm using Scherrer formula.

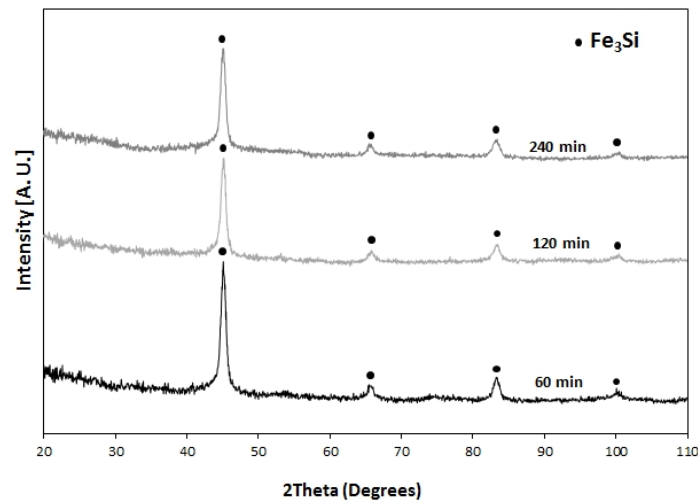


Fig 8. XRD multiplot patterns of the simultaneously annealed and coated Finemet foils for 60, 120 and 240 minutes

In nanocrystalline Finemet materials, obtaining grain sizes in the range of 10-15nm is of great importance. In these alloys, if the grain size is reduced to less than about 35nm, the magnetization will not follow the randomly oriented easy axis of individual grains and is forced to align parallel by exchange interaction. As a result, the effective anisotropy is an average over some grains and reduced in magnitude. When the grain sizes are in the order of 10-15 nm, the magnetocrystalline anisotropy is

reduced towards a few J/m^3 , i.e. small enough to obtain superior soft magnetic properties [10].

The thickness of the coating formed on nanocrystalline foils was measured using FESEM. Cross sectional FESEM images of the wheel contact and free surfaces of the heat treated foils for 60, 120 and 240 minutes are presented in Fig. 9. As expected, the coating thickness of both surfaces is increased with the heat treatment time. The average coating thicknesses formed on both surfaces of nanocrystalline foils are given in Table 1.

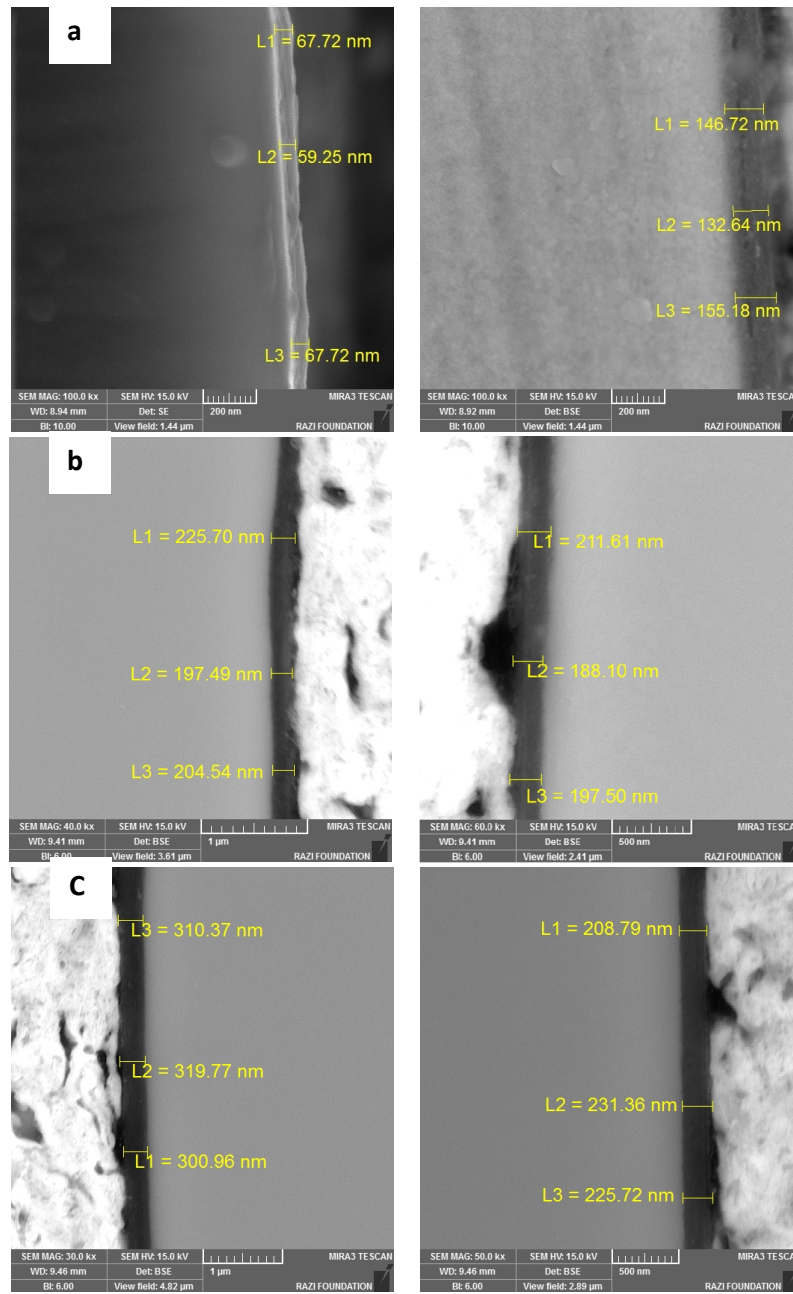


Fig 9. Cross sectional FESEM images of the wheel contact (left) and free (right) surfaces of the heat treated foils for: a) 60, b) 120 and c) 240 minutes

Table 1. Average coating thicknesses of the wheel contact and free surfaces of the nanocrystalline Finemet foils

Heat-treatment (Coating) Time (minutes)	Coating Thickness of Wheel Contact Surface (nm)	Coating Thickness of Free Surface (nm)
60	65	145
120	209	199
240	310	222

In order to characterize the chemical composition of the coating layer, the free surface of the foils heat treated for 60, 120 and 240

minutes were analyzed by FESEM-EDS method and the results are listed in Table 2.

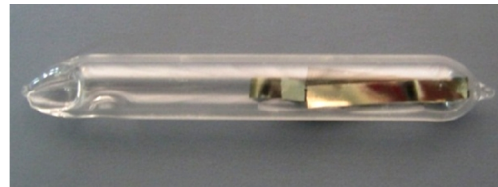
Table 2. FESEM-EDS analysis of the free surfaces of the uncoated nanocrystalline foil and the coated nanocrystalline foils heat treated for 60, 120 and 240 minutes

Element	Atomic Percent				Weight Percent			
	Uncoated	60min	120min	240min	Uncoated	60min	120min	240min
O	11.08	42.46	46.26	52.76	3.61	18.12	20.54	25.15
Si	13.00	8.18	7.94	7.12	7.43	6.13	6.19	5.95
Fe	71.76	46.72	43.13	37.80	81.55	69.61	66.85	62.91
Cu	0.77	0.55	0.57	0.50	0.99	0.93	1.00	0.95
Nb	3.40	2.10	2.10	1.82	6.42	5.22	5.42	5.04

* Measurement of boron content was not possible by EDS analysis

As presented in Table 2, an increase in the heat treatment time leads to an increase in the oxygen content and a decrease in iron, silicon and niobium percentages. In the other words, simultaneous annealing and oxidation of Finemet foils results in the appearance of iron-, silicon- and niobium oxides on the surface of nanocrystalline Finemet foils.

Since the FESEM-EDS results are not conclusive for exact identification of the coating layer composition, the GI-XRD and FTIR analyses were used for a detailed identification. GI-XRD is used to characterize structural features such as phases, crystallite sizes and stresses in thin films, multilayer systems and coatings. For precise determination of the coating chemical composition and omission of the substrate (nanocrystalline foil) phases, amorphous Finemet foils were encapsulated in a quartz tube under vacuum (10^{-5} mbar) and annealed in a tube furnace (Fig. 10).

**Fig 10.** Finemet foils encapsulated in a quartz tube

The GI-XRD patterns of the heat treated foils for 60, 120 and 240 minutes are presented in Figs. 11-13, respectively. According to the GI-XRD results, after annealing and oxidation of Finemet foils for 60 minutes, SiO_2 and Fe_3O_4 oxides develop in the coating layer. By increasing the heat treatment time to 120 minutes, Fe_2O_3 , NbO_2 , B_2O_3 and SiO_2 phases are formed and further increasing of the heat treatment time to 240 minutes results in the formation of SiO_2 , B_2O_3 , NbO_2 and Nb_2O_5 phases on the foil surfaces.

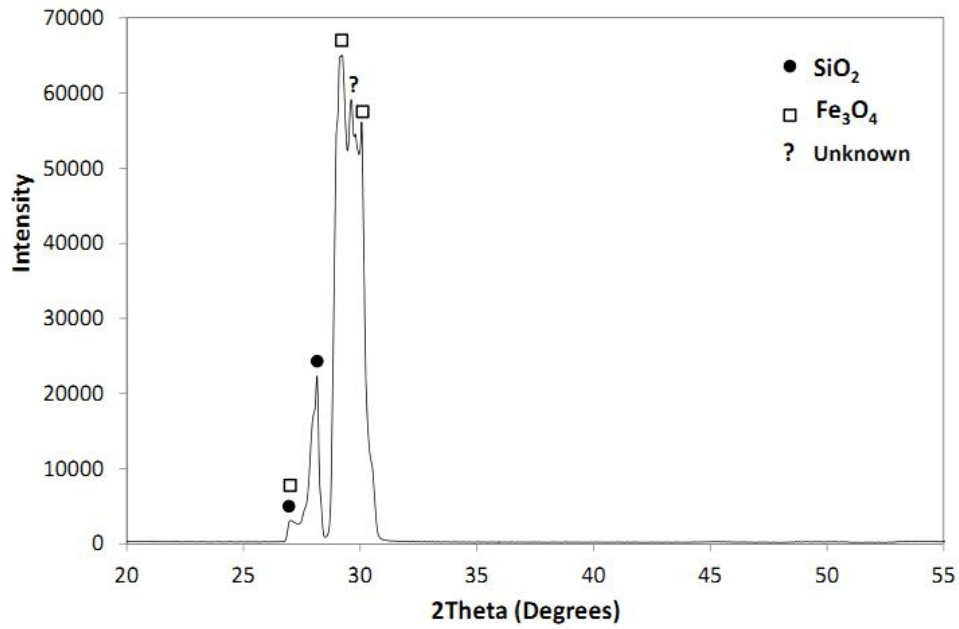


Fig 11. GI-XRD patterns of the simultaneously annealed and oxidized foil for 60 minutes

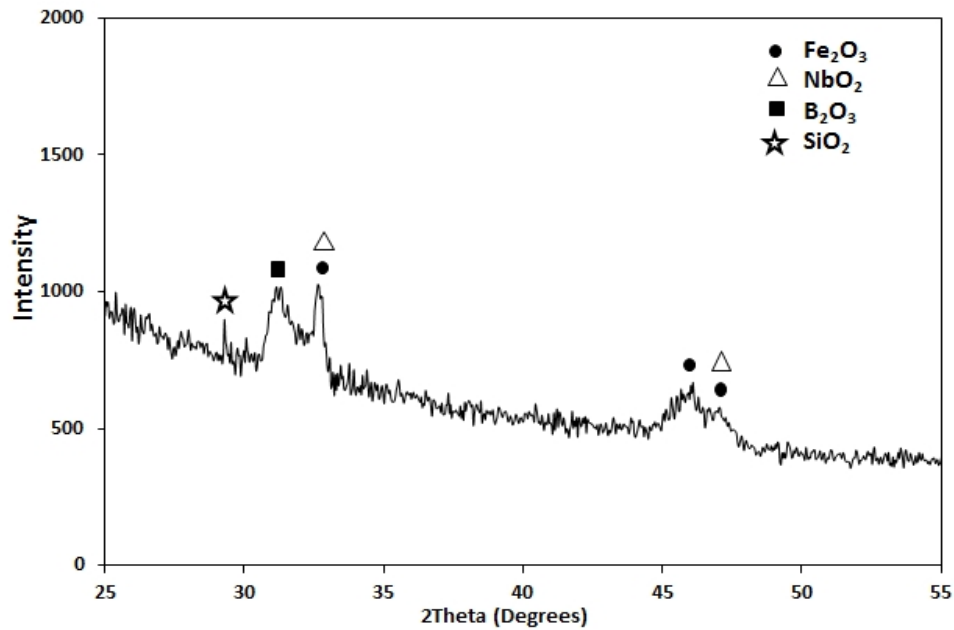


Fig 12. GI-XRD patterns of the simultaneously annealed and oxidized foil for 120 minutes

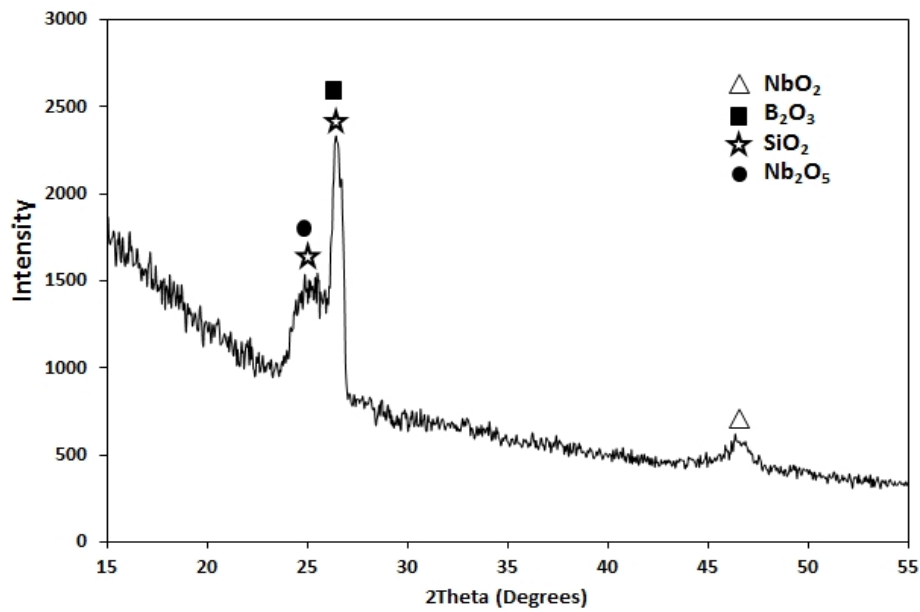


Fig 13. GI-XRD patterns of simultaneously annealed and oxidized foil for 240 minutes.

Fig. 14 shows the experimental FTIR spectra obtained from the air side of the heat treated foils for 60, 120 and 240 minutes. As illustrated in Fig. 14, FTIR results confirm the formation of silicon-, boron- and niobium oxides on the surface of nanocrystalline Finemet foils. The observed bands and their assignments along

with the literature data are summarized in Table 3. The obtained peaks were slightly shifted in comparison to the literature data. This can be clarified by the presence of other ions in the coating layer due to the alloying elements in the substrate (nanocrystalline foil) [11].

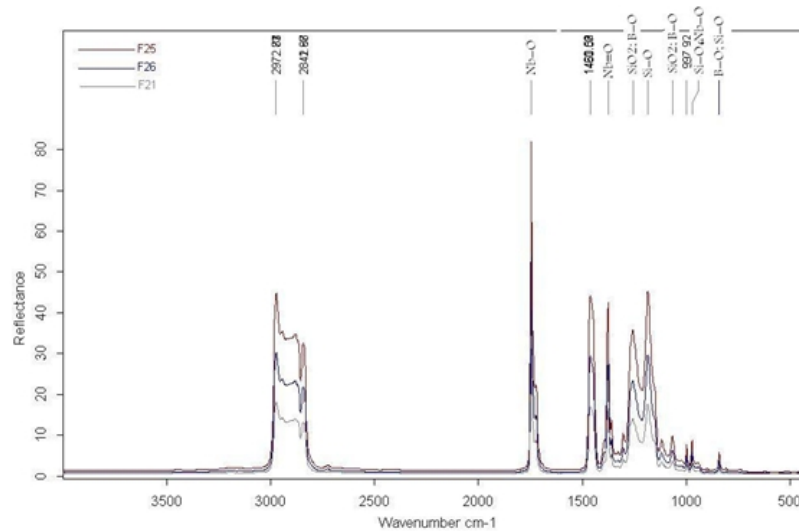


Fig 14. FTIR spectra from air side (free surface) of the foils heat treated for 60, 120 and 240 minutes

Table 3. Wave numbers and their assignments for FTIR spectra of the heat treated Finemet foils

Observed Bands (cm ⁻¹)	Band Assignment	Literature Data (cm ⁻¹)
840, 1065, 1256	B-O	875, 1050, 1250 [12]
840, 972, 1184	Si-O	800, 930, 1123 [13, 14]
972, 1745	Nb-O	930, 1174 [14, 15]
1377	Nb=O	1380 [14]
1065, 1256	SiO ₂	1072, 1250 [16]

3.4. Magnetic Properties

Magnetic properties of the amorphous and heat treated foils for 60, 120 and 240 minutes are given in Table 4. It can be concluded that the soft magnetic properties of heat treated foils have significantly improved compared to the

amorphous state. In other words, simultaneous annealing and oxidation of amorphous Finemet foils caused an increase in saturation induction, initial permeability and maximum permeability as well as a decrease in hysteresis loss.

Table 4. Magnetic properties of amorphous and heat treated foils for 60, 120 and 240 minutes

Heat Treatment Time (minutes)	Coercivity H _C (A/m)	Saturation Induction, B _S (mT)	Hysteresis Loss (J/m ³)	Initial Permeability μ _{r(i)}	Maximum Permeability μ _{r(m)}
0 (as-spun)	3.04	792	16.37	2025	90798
60	2.97	1219	20.47	17610	131462
120	2.97	1290	13.63	51089	103292
240	3.46	1213	16.3	29531	102575

4. Conclusion

In the present research, wound cores of amorphous Finemet foils were simultaneously annealed and heat treated at 540°C in steam and air flow to form oxide insulating coating layer on both surfaces of the foils and the following results were obtained:

1- The XRD patterns for both surfaces of the as-spun Finemet foils exhibited only one broad peak around 2θ≈45°, indicating that the structure of as-quenched foil is fully amorphous.

2- Upon simultaneous annealing and oxidizing processes, the amorphous structure of the foil was transformed into nanocrystalline state with a grain size in the range of 10-12 nm and an oxide coating was formed on both surfaces of the foils.

3- The formation of Fe₃Si nanocrystals caused an increase in the saturation induction, initial permeability, and maximum permeability as well as a decrease in the hysteresis loss.

4- The coating thickness formed on air and wheel surfaces of the nanocrystalline foil was in the range of 65-310 nm and these coating layers

contained a mixture of iron, silicon, boron, and niobium oxides.

References

1. Yoshizawa, Y., Oguma, S., Yamauchi, K., 1988a. New Fe-Based Soft Magnetic-Alloys Composed of Ultrafine Grain-Structure. *J. Appl. Phys.* 64, 6044.
2. Willard M. A. and Daniil M., "Nanocrystalline Soft Magnetic Alloys Two Decades of Progress", *Handbook of Magnetic Materials*, Vol. 21, Elsevier Science, 2013, pp. 173-342.
3. Wood, R., Lathlaen, R. and Beckham, W. C., "Magnetic Core Insulation", United States Patent No. US 2004/0007291 A1, Jan. 15, 2004.
4. Hasegawa, R. and Kroger, C. E., "Magnetic Implement Using Magnetic Metal Ribbon Coated with Insulator", United States Patent No. US 2005/0221126 A1, Oct. 6, 2005.
5. Mirzaei, S., "Production of Nanocrystalline Transformer Cores in Laboratory Scale", Research Project, Technology Development

- Institute, Sharif Branch of ACECR, July 2015 (in Persian).
6. Shahri, F., Beitollahi, A., Shabestari, S.G., Ghanaatshoar, M., Tehranchi, M.M., Mohseni, S.M., Roozmeh, S.E., Wanderka, N. and Fiorillo, F., "Structural characterization and magnetoimpedance effect in amorphous and nanocrystalline AlGe-substituted FeSiBNbCu ribbons", *J. Magn. Mater.*, Vol. 312, 2007, pp. 35–42.
 7. Hosseini-Nasb, F., Beitollahi, A. and Moravvej-Farshi, M.K., "Effect of crystallization on soft magnetic properties of nanocrystalline Fe₈₀B₁₀Si₈Nb₁Cu₁ alloy", *J. Magn. Mater.*, Vol. 373, 2015, pp. 255–258.
 8. Sohrabi, S., Arabi, H., Beitollahi, A. and Gholamipour, R., "Planar Flow Casting of Fe₇₁Si_{13.5}B₉Nb₃Cu₁Al_{1.5}Ge₁ Ribbons", *J. Mater. Eng. Perform.*, Vol. 22, Issue 8, 2013, pp. 2185-2190.
 9. Jazayeri Gharehbagh, A., Molla, J., Esfahani, M., Binesh, B., Kiani, M., Mirzaei, S., Arouni, H., Bakhtiari, R. and Parvizi, S., "Rapid Solidification Processing and Its Application in Production of Amorphous and Nanocrystalline Materials", 1st ed., Sharif Branch of ACECR, 2011 (in Persian).
 10. Herzer, G., "Nanocrystalline Soft Magnetic Alloys", *Handbook of Magnetic Materials*, Vol. 10, Elsevier Science, 1997.
 11. Vishwanadh, B., Balasubramaniam, R., Srivastava, D. and DEY, G. K., "Effect of Surface Morphology on Atmospheric Corrosion Behaviour of Fe-based Metallic Glass, Fe₆₇Co₁₈Si₁₄B₁", *Bull. Mater. Sci.*, Vol. 31, No. 4, 2008, pp. 693–698.
 12. Pascuta, P., Borodi, G., Bosca, M., Pop, L., Rada, S. and Culea, E., "Preparation and Structural Characterization of Some Fe₂O₃-B₂O₃-ZnO Glasses and Glass Ceramics", *J. Phys.: Conf. Ser.*, Vol. 182, 2009, 012072.
 13. Serra, J., Gonzalez, P., Liste, S., Serra, C., Chiussi, S., Leon, B., Perez-Amor, M., Ylanen, H.O., Hupa, M., "FTIR and XPS Studies of Bioactive Silica Based Glasses", *J. Non-Cryst. Solids*, Vol. 332, 2003, pp. 20–27.
 14. Pernice, P., Aronne, A., Sigaev, V., Kupriyanova, M., "Crystallization of the K₂O.Nb₂O₅.2SiO₂ Glass: Evidences for Existence of Bulk Nanocrystalline Structure", *J. Non-Cryst. Solids*, Vol. 275, 2000, pp. 216-224.
 15. Bhagavannarayana, G., Ananthamurthy, R. V., Budakoti, G. C., Kumar, B. and Bartwal, K. S., "A study of the effect of annealing on Fe-doped LiNbO₃ by HRXRD, XRT and FT-IR", *J. Appl. Cryst.*, Vol. 38, 2005, pp. 768–771.
 16. Tolstoy, V. P., Chernyshova, I. V. and Skryshevsky, V. A., "Handbook of Infrared Spectroscopy of Ultrathin Films", John Wiley & Sons, Inc., Hoboken, New Jersey, 2003.